

# Online Research @ Cardiff

This is an Open Access document downloaded from ORCA, Cardiff University's institutional repository: <https://orca.cardiff.ac.uk/id/eprint/113719/>

This is the author's version of a work that was submitted to / accepted for publication.

Citation for final published version:

Mehellou, Youcef ORCID: <https://orcid.org/0000-0001-5720-8513>, Alamri, Mubarak A., Dhiani, Binar A. and Kadri, Hachemi 2018. C-terminal phosphorylation of SPAK and OSR1 kinases promotes their binding and activation by the scaffolding protein MO25. Biochemical and Biophysical Research Communications 503 (3) , pp. 1868-1873.  
10.1016/j.bbrc.2018.07.128 file

Publishers page: <http://dx.doi.org/10.1016/j.bbrc.2018.07.128>  
<<http://dx.doi.org/10.1016/j.bbrc.2018.07.128>>

Please note:

Changes made as a result of publishing processes such as copy-editing, formatting and page numbers may not be reflected in this version. For the definitive version of this publication, please refer to the published source. You are advised to consult the publisher's version if you wish to cite this paper.

This version is being made available in accordance with publisher policies.

See

<http://orca.cf.ac.uk/policies.html> for usage policies. Copyright and moral rights for publications made available in ORCA are retained by the copyright holders.



# **C-terminal Phosphorylation of SPAK and OSR1 Kinases Promotes Their Binding and Activation by the Scaffolding Protein MO25**

Youcef Mehellou,<sup>1,\*</sup> Mubarak A. Alamari,<sup>2</sup> Binar A. Dhiani,<sup>1</sup> Hachemi Kadri<sup>1</sup>

<sup>1</sup>School of Pharmacy and Pharmaceutical Sciences, King Edward VII Avenue, Cardiff University,  
Cardiff CF10 3NB, UK.

<sup>2</sup>School of Pharmacy, College of Medical and Dental Sciences, University of Birmingham, Edgbaston,  
Birmingham B15 2TT, UK.

\*Correspondence: Tel: +44 (0) 2920875821. Email: [MehellouY1@cardiff.ac.uk](mailto:MehellouY1@cardiff.ac.uk).

## **Abstract**

SPAK and OSR1 are two protein kinases that play important roles in regulating the function of numerous ion co-transporters. They are activated by two distinct mechanisms that involve initial phosphorylation at their T-loops by WNK kinases and subsequent binding to a scaffolding protein termed MO25. To understand this latter SPAK and OSR1 regulation mechanism, we herein show that MO25 binding to these two kinases is enhanced by serine phosphorylation in their highly conserved WEWS motif, which is located in their C-terminal domains. Furthermore, we show that this C-terminal phosphorylation is carried out by WNK kinases *in vitro* and involves WNK kinases in cells. Mutagenesis studies revealed key MO25 residues that are important for MO25 binding and activation of SPAK and OSR1 kinases. Collectively, this study provides new insights into the MO25-mediated activation of SPAK and OSR1 kinases, which are emerging as important players in regulating ion homeostasis.

**Keywords:** SPAK, OSR1, Kinase, MO25, Phosphorylation.

## 1. Introduction

Ste20-related proline-alanine-rich kinase (SPAK) and oxidative-stress-responsive kinase 1 (OSR1) are two serine/threonine protein kinases that are involved in the regulation of cellular ion homeostasis [1, 2]. The amino acid sequences of SPAK and OSR1 are 68% identical and share a highly conserved 92-amino acids C-terminal (CCT) domain that mediates their binding to upstream and downstream protein partners [3] (**Figure 1A**). The involvement of SPAK and OSR1 kinases in regulating ion homeostasis is a result of their ability to manipulate the function of a series of sodium, potassium and chloride ion co-transporters, such as NKCC1 and 2, NCC and KCC [1, 2] (**Figure 1A**), which regulate blood pressure [4]. The activation of SPAK and OSR1 kinases is triggered by phosphorylation at their T-loops, T-185 for OSR1 and T233 for SPAK (**Figure 1A**), by the WNK family of protein kinases [5] whose mutations cause hypertension in humans [6]. Beyond T-loop phosphorylation, WNK kinases are known to phosphorylate SPAK and OSR1 at serine residues on their C-terminal motif ([www.phosphosite.org](http://www.phosphosite.org)) though the roles of such phosphorylation remains unclear. The catalytic activity of WNK-phosphorylated SPAK and OSR1 kinases is further enhanced by binding to a scaffolding protein known as mouse protein 25 (MO25) [7]. In humans, two isoforms ( $\alpha$ - and  $\beta$ -) of MO25, which share 79% sequence identity, exist and they form key components of numerous protein complexes that perform diverse biological functions [8]. The binding of MO25 to WNK-phosphorylated SPAK and OSR1 kinases leads to 80- to 100-fold increase in their *in vitro* catalytic activity, respectively [7]. In cells, siRNA knock-down of MO25 $\alpha$  resulted in a significant reduction in SPAK and OSR1 phosphorylation of their physiological substrate NKCC1 [7].

Beyond binding to SPAK and OSR1 kinases, MO25 $\alpha$  along with the pseudokinase STRAD $\alpha$  forms a heterotrimeric complex with the tumor suppressor kinase LKB1 [9] that phosphorylates numerous AMPK-related kinases [10, 11]. The crystal structure of this heterotrimeric protein complex [12] as well as that of MO25 $\alpha$  in complex with STRAD $\alpha$  [13] shows that one of the key regions of STRAD $\alpha$  that is responsible for binding to MO25 is a C-terminal region that contains a WEF motif. Indeed, mutations in the WEF motif of STRAD $\alpha$  resulted in a loss of binding to MO25 $\alpha$  [12]. Sequence alignment of human SPAK and OSR1 kinases with human STRAD $\alpha$  shows the WEF motif of STRAD $\alpha$  (aa. 329-431) aligns perfectly with a conserved WEW motif on SPAK and OSR1 kinases, aa. 384-386 and 336-338, respectively (**Supplementary Figure S1**) [7]. We previously showed that the WEW motif of SPAK and OSR1 was essential in binding MO25 as mutations in either tryptophan (W) residues in this motif resulted in a significant loss of binding to MO25 that was translated into poor activation of SPAK and OSR1 [7]. The WEW motif of SPAK and OSR1 kinases is followed immediately by a serine residue while for STRAD $\alpha$  such residue was not present as the WEF was the final motif of the protein sequence.

Given that this serine residue is reported to get phosphorylated ([www.phosphosite.org](http://www.phosphosite.org)), we were intrigued by the possible impact of this phosphorylation on MO25 binding to SPAK and OSR1.

## **2. Material and Methods**

### *2.1. Reagents and standard experimental procedures*

Detailed reagents and general experimental procedures such as immunoblotting and *in vitro* kinase assays are provided in the Supplementary Data.

### *2.2. Peptide pull-down and MS analysis*

Cell lysates from HEK293 cells were centrifuged for 15 min at 14,000 rpm at 4 °C and the protein concentration was determined by Bradford. 15 mg of total protein lysate was precleared incubated 3 times with 15  $\mu$ L of streptavidin beads. 3 mg of the precleared lysate was incubated with 3  $\mu$ g of each of the following peptides: biotin-C<sub>12</sub>-TEDGDWEWSDDDEMDEK, biotin-C<sub>12</sub>-TEDGDWEWS\*DDEMDEK or biotin-C<sub>6</sub>-SEEGKPQLVGRFQVTSSK for 10 min at 4 °C under gentle agitation. This was followed by the addition of 15  $\mu$ L of Streptavidin-Sepharose (pre-equilibrated in lysis buffer) slurry beads to every sample. As a reference, 3 mg of the precleared lysate was also incubated with 15  $\mu$ L of Streptavidin-Sepharose (pre-equilibrated in lysis buffer) slurry beads. After further 5 min incubation at 4 °C under gentle agitation, the sample was centrifuged for at 5,000 rpm at 4 °C for 2 min. The beads were subsequently washed twice with lysis buffer and twice with buffer A. The beads were then suspended in 40  $\mu$ L of 1x SDS sample buffer, subjected to electrophoresis on a precast 4–12% gradient gel (Invitrogen) and the protein bands were visualized following Colloidal Blue staining. Proteins in the selected gel bands were reduced and alkylated by the addition of 10 mM DTT, followed by 50 mM iodoacetamide. Identification of proteins was performed by in-gel digestion of the proteins with 5  $\mu$ g/mL trypsin and subsequent analysis of the tryptic peptides by LC (liquid chromatography)–MS/MS (tandem MS) on a Thermo LTQ-Orbitrap system coupled to a Thermo Easy nano-LC instrument. Excalibur RAW files were converted into peak lists by Raw2msm[14] and then analysed by Mascot (<http://www.matrixscience.com>), utilizing the SwissProt human database. Two missed cleavages were permitted, the significance threshold was  $P < 0.05$ .

### *2.3. Fluorescence polarisation (FP) assay*

The peptides used for the fluorescence polarisation (FP) assay were CCPGCCGGTEDGDWEWSDDDEMDEK and CCPGCCGGTEDGDWEWpSDDDEMDEK. The peptides were labelled with Lumio Green (Invitrogen) following the manufacturer's protocol. Fluorescence polarization measurements were performed at room temperature in buffer containing 50 mM TrisHCl (pH 7.5), 200 mM NaCl and 5 mM DTT. Binding assays were performed by combining 10 nM labelled peptide with increasing concentrations of MO25 $\alpha$ , in a total volume of 60  $\mu$ L of buffer, and end-point polarization measurements were made using the BMG PheraStar plate reader. The polarization values

were measured at an excitation wavelength of 485 nm and an emission wavelength of 538 nm, and were corrected for fluorescent probe alone. All data points were measured in triplicates. The data was analysed using GraphPad Prism 5 and curve-fitting of the data from two independent experiments was performed with one-site specific binding with Hill slope [model  $Y = B_{\max}X^h/(K_d^h + X^h)$ ] to determine  $K_d$  values as reported[15].

#### 2.4. Pulldown and peptide competition assay

Wild-type (WT) Myc-tagged MO25 $\alpha$  or the indicated mutants were overexpressed in HEK293 cells. Cell lysates (3 mg) were treated with 3  $\mu$ g of biotinylated peptides [either phosphorylated (Biotin-C<sub>12</sub>-TEDGDWEWpSDDEMDEK) or non-phosphorylated (Biotin-C<sub>12</sub>-TEDGDWEWSDDDEMDEK)]. Following streptavidin-biotin pull down and washing twice with lysis buffer and twice with buffer A, the material underwent blotting for Myc.

#### 2.5. In silico docking

Autodock Vina 1.1.2[16] was used for docking of WEW tripeptide into the human MO25 $\alpha$  crystal structure (PDB: 1UPK) [17]. Initially, Discovery Studio 4.5 program (Accelrys, San Diego, CA, USA) was used to prepare the pdb files of MO25 protein, WEF and WEW peptides. AutoDock Tool 1.5.6 program was used to convert pdb files into pdbqt format [18]. The Grid box was set to cover the binding site of WEF using the following coordination in the Configuration input file (size\_x = 18 size\_y = 14 size\_z = 16 center\_x = 59.026 center\_y = -41.500 center\_z = 4.568). The docking results were visualized and analyzed using PyMOL Molecular Graphics System 1.3.

### 3. Results and Discussion

#### 3.1. Serine phosphorylation of SPAK and OSR1 in the WEWS motif increases MO25 binding

In order to examine the importance of the conserved serine residue in the WEWS motif of SPAK and OSR1, we synthesised two 16-mer biotinylated peptides (biotin-C<sub>12</sub>-TEDGDWEWSSDDDEMDEK) corresponding to amino acid residues 379-394 of human SPAK where in one peptide the serine residue adjacent to the WEWS motif was phosphorylated while it was unphosphorylated in the second peptide. In addition, we also synthesised an 18-mer biotinylated peptide biotin-C<sub>12</sub>-SEEGKPQLVGRRFQVTSSK (RFQV peptide) derived from WNK1 (aa. 1006-1023), which we had previously shown that it binds to endogenous SPAK and OSR1 [3]. We subsequently incubated these peptides with HEK293 cell lysates, which endogenously express MO25. Upon streptavidin-biotin pull down, the isolated material from each sample was analysed by mass spec to identify the proteins that bound each peptide (**Figure 1A**). The material pulled down by the 18-mer RFQV peptide led to the precipitation of endogenous SPAK and OSR1 as expected [3]. Interestingly, the mass spec data showed that the 16-mer WEW peptide derived from SPAK, which had the serine residue phosphorylated,

pulled down endogenous MO25 while its unphosphorylated peptide counterpart did not (**Figure 1B** and **1C**). To investigate this finding further, we repeated the streptavidin-biotin pull down from HEK293 cell lysates using the three different peptides and performed western blotting using SPAK and MO25 antibodies. The data showed that the positive control (18-mer RFQV) pulled down endogenous SPAK, while none of the other two 18-mer WEW peptides did (**Figure 1D**). Strikingly, the peptide derived from SPAK bearing the phosphorylated serine residue within the WEWS motif pulled down a significantly larger amount endogenous MO25 as compared to the unphosphorylated peptide counterpart (**Figure 1D**).

In order to measure the effect of SPAK S387 phosphorylation on MO25 binding, we developed a fluorescence polarisation (FP) assay that measures the binding affinity of the peptide derived from SPAK with S387 phosphorylated and that in which the same serine residue was not phosphorylated. The data showed that the peptide derived from SPAK in which S387 was phosphorylated had a higher affinity ( $K_D = 4.91 \mu\text{M}$ ) for MO25 than its unphosphorylated counterpart ( $K_D = 16.04 \mu\text{M}$ ) (**Figure 1D**). This ca. 4-fold difference in binding affinity correlates with the results from the pull-down assay (**Figure 1C**). Collectively, this data indicates that phosphorylation of SPAK at S387 enhances binding to MO25.

### *3.2. SPAK is phosphorylated at S387 in vitro and is not an autophosphorylation site*

After establishing the role of SPAK phosphorylation at S387 in binding to MO25, we next investigated the possibility of SPAK S387 phosphorylation being carried out by WNK kinases. It is well known that WNK kinases phosphorylate SPAK at S373 on its C-terminal domain [5], but there have been no reports on WNK kinases phosphorylating SPAK at S387. To address this, we initially performed an *in vitro* kinase assay using recombinant WNK1 (1-667) and SPAK WT followed by western blotting for SPAK S373 and S387. The data showed that SPAK was phosphorylated *in vitro* by WNK1 at T233 and S373 as reported previously (**Figure 2**) [5]. Interestingly, the data also showed that WNK kinases phosphorylated SPAK at S387. In addition, the data presented in **Figure 2** shows WNK1 WT was able to phosphorylate the three sites on SPAK WT and SPAK kinase-dead (KD) as expected. However, no phosphorylation of any of the three residues was detected when WNK1 KD was incubated with SPAK WT confirming that none of these three phosphorylation sites, including the newly identified SPAK S387, are autophosphorylation sites.

### *3.3. SPAK S387 is phosphorylation is WNK-dependent in cells*

In order to determine if SPAK was phosphorylated at residue S387 by WNK kinases in cells, we stimulated HEK293 cells, which express endogenously the WNK-SPAK/OSR1-MO25 signalling components, with hypotonic buffer or sorbitol for different periods of time. Both hypotonic buffer and sorbitol has been shown to activate WNK-SPAK/OSR1 signalling in cells [14]. Upon cell lysis, the lysates were subjected to western blotting for SPAK S-motif phosphorylation; S373 and S387. As

shown in **Figure 3A**, the data shows that the treatment of HEK293 cells with either sorbitol or hypotonic buffer resulted in the phosphorylation of SPAK at S373, as has been shown before [14]. Interestingly, the data also shows that SPAK was also phosphorylated at S387 following HEK293 cells stimulation by hypotonic buffer or sorbitol. This suggests that SPAK S387 phosphorylation is likely to be carried out in a WNK-dependent manner. Notably, OSR1 S339, which falls immediately after the WEW motif and aligns with SPAK S387, was reported to be directly phosphorylated by mTORC2 though the function of this phosphorylation site was not extensively studied [19]. To investigate whether the hypotonic buffer mediated phosphorylation of SPAK S387 that we observed in **Figure 3A** is WNK- or mTORC2 phosphorylation, we repeated the experiment using the specific WNK inhibitor, WNK463 [20], and the mTORC2 inhibitor AZD8055 [21]. Confluent HEK293 cells were firstly treated with hypotonic buffer to activate WNK-signalling and then treated with varying concentrations of WNK463 or AZD8055. The results showed that WNK463 inhibited SPAK S373 phosphorylation in a concentration dependent manner as expected while AZD8055 had no effect on such phosphorylation (**Figure 3B**). Also, AZD8055 inhibited mTORC2 phosphorylation of AKT at S473 whereas WNK463 had no effect on AKT phosphorylation by mTORC2 (**Figure 3B**). Interestingly, cell treatment with WNK463 also led to a dose-dependent reduction of SPAK S387 phosphorylation while the mTORC2 inhibitor AZD8055 did not suppress SPAK S387 phosphorylation (**Figure 3B**). This indicated that SPAK S387 phosphorylation is likely to be WNK-dependent.

### 3.2. Mapping the interaction between SPAK/OSR1 and MO25

In order to understand where the conserved WEWS motif of SPAK and OSR1 binds to MO25, we performed *in silico* docking studies of the WEW motif into the crystal structure of MO25 $\alpha$  (PDB: 1UPK). The docking revealed the WEW motif from SPAK/OSR1 docked in the same pocket on MO25 $\alpha$  where the WEF of the pseudokinase STRAD $\alpha$  was found to bind (**Figure 4A-C**) [17]. This pocket had four key amino acid residues (K257, R264, K297 and K301), which appear to form interactions with the WEW motif (**Figure 4A-C**). Notably, these same amino acids were verified previously as being important in binding STRAD $\alpha$  [17]. To verify the obtained docking poses and the importance of these four amino acids, we mutated these MO25 $\alpha$  residues and studied their effect on the MO25-dependent activation of SPAK and OSR1 kinases. Indeed, Myc-tagged MO25 $\alpha$  mutants K257M, K257F, R264A, K297M and K301M were cloned, expressed in *E.coli* (**Supplementary Figure S2**) and studied their effect on the activation of SPAK T233E and OSR1 T185E *in vitro* using kinase assays as previously reported [7, 22]. We used SPAK T233E and OSR1 T185E instead of SPAK WT and OSR1 WT as the glutamic acids mutants are introduced to mimic phosphorylation of these residues by WNK kinases [5]. The data shown in **Figure 4D** and **E** reveals that mutating K301 to methionine (M) has the strongest effect on reducing the MO25-dependent activation of SPAK and OSR1. This was followed by mutating K257 to

phenylalanine (F) while mutating this residue to a less bulkier amino acid, methionine (M) in this case, did not have as a significant effect as mutating it to methionine (M). Interestingly, mutations of R264 and K297 had little effect on the MO25-dependent activation of SPAK and OSR1 *in vitro*.

To explore the binding of these MO25 $\alpha$  mutations to the phosphorylated and unphosphorylated SPAK/OSR1 WEWS motif, we overexpressed the MO25 $\alpha$  Myc-tagged mutants (K257M, K257F, R264A, K297M and K301M) in HEK293 cells (**Supplementary Figure S3**). 200  $\mu$ g from each cell lysate was incubated with 3  $\mu$ g of either biotin-C<sub>12</sub>-TEDGDWEWSDDDEMDEK or biotin-C<sub>12</sub>-TEDGDWEWpSDDDEMDEK. Following streptavidin-biotin, pull down the material underwent blotting for Myc. As shown in **Figure 4F**, the phosphorylated WEWS peptide pulled down a more significant MO25 $\alpha$  WT than its unphosphorylated counterpart. This is in agreement with the data shown in **Figure 1D**. Interestingly, none of the other mutants were found to be pulled down by either the phosphorylated or unphosphorylated WEWS peptides. The only exception is the K297M mutant, which seemed to bind the phosphorylated and unphosphorylated WEWS peptides in almost the same amount, though this was still significantly lower than the binding of the phosphorylated peptide to the MO25 $\alpha$  WT. Together the data shows that K257 and K301 of MO25 $\alpha$  play an important role in binding SPAK and OSR1 kinases.

In conclusion, we demonstrated that phosphorylation of SPAK and OSR1 in the serine residue adjacent to the WEW motif enhances binding to MO25. This serine phosphorylation is not an autophosphorylation site and in cells it is carried out in WNK-dependent manner. Furthermore, mutagenesis studies indicated key MO25 $\alpha$  residues that are important for mediating the binding to SPAK/OSR1 kinases and their activation. Collectively, this work identifies an important role for the serine residue of the WEWS motif in the regulation of the catalytic activity of SPAK and OSR1 kinases by the scaffolding protein MO25.

## References

- [1] D.R. Alessi, J. Zhang, A. Khanna, T. Hochdorfer, Y. Shang, K.T. Kahle, The WNK-SPAK/OSR1 pathway: master regulator of cation-chloride cotransporters, *Sci. Signal.* 7 (2014) re3.
- [2] J. Hadchouel, D.H. Ellison, G. Gamba, Regulation of Renal Electrolyte Transport by WNK and SPAK-OSR1 Kinases, *Annu. Rev. Physiol.* 78 (2016) 367-389.
- [3] A.C. Vitari, J. Thastrup, F.H. Rafiqi, M. Deak, N.A. Morrice, H.K. Karlsson, D.R. Alessi, Functional interactions of the SPAK/OSR1 kinases with their upstream activator WNK1 and downstream substrate NKCC1, *Biochem. J.* 397 (2006) 223-231.
- [4] M. Murthy, T. Kurz, K.M. O'Shaughnessy, WNK signalling pathways in blood pressure regulation, *Cell. Mol. Life Sci.* 74 (2017) 1261-1280.



- [5] A.C. Vitari, M. Deak, N.A. Morrice, D.R. Alessi, The WNK1 and WNK4 protein kinases that are mutated in Gordon's hypertension syndrome phosphorylate and activate SPAK and OSR1 protein kinases, *Biochem. J.* 391 (2005) 17-24.
- [6] F.H. Wilson, S. Disse-Nicodeme, K.A. Choate, K. Ishikawa, C. Nelson-Williams, I. Desitter, M. Gunel, D.V. Milford, G.W. Lipkin, J.M. Achard, M.P. Feely, B. Dussol, Y. Berland, R.J. Unwin, H. Mayan, D.B. Simon, Z. Farfel, X. Jeunemaitre, R.P. Lifton, Human hypertension caused by mutations in WNK kinases, *Science* 293 (2001) 1107-1112.
- [7] B.M. Filippi, P. de los Heros, Y. Mehellou, I. Navratilova, R. Gourlay, M. Deak, L. Plater, R. Toth, E. Zeqiraj, D.R. Alessi, MO25 is a master regulator of SPAK/OSR1 and MST3/MST4/YSK1 protein kinases, *EMBO J.* 30 (2011) 1730-1741.
- [8] J. Boudeau, A.F. Baas, M. Deak, N.A. Morrice, A. Kieloch, M. Schutkowski, A.R. Prescott, H.C. Clevers, D.R. Alessi, MO25 $\alpha$ /beta interact with STRAD $\alpha$ /beta enhancing their ability to bind, activate and localize LKB1 in the cytoplasm, *EMBO J.* 22 (2003) 5102-5114.
- [9] J. Boudeau, J.W. Scott, N. Resta, M. Deak, A. Kieloch, D. Komander, D.G. Hardie, A.R. Prescott, D.M. van Aalten, D.R. Alessi, Analysis of the LKB1-STRAD-MO25 complex, *J. Cell Sci.* 117 (2004) 6365-6375.
- [10] J.M. Lizcano, O. Goransson, R. Toth, M. Deak, N.A. Morrice, J. Boudeau, S.A. Hawley, L. Udd, T.P. Makela, D.G. Hardie, D.R. Alessi, LKB1 is a master kinase that activates 13 kinases of the AMPK subfamily, including MARK/PAR-1, *EMBO J.* 23 (2004) 833-843.
- [11] S.A. Hawley, J. Boudeau, J.L. Reid, K.J. Mustard, L. Udd, T.P. Makela, D.R. Alessi, D.G. Hardie, Complexes between the LKB1 tumor suppressor, STRAD  $\alpha$ /beta and MO25  $\alpha$ /beta are upstream kinases in the AMP-activated protein kinase cascade, *J. Biol.* 2 (2003) 28.
- [12] E. Zeqiraj, B.M. Filippi, M. Deak, D.R. Alessi, D.M. van Aalten, Structure of the LKB1-STRAD-MO25 complex reveals an allosteric mechanism of kinase activation, *Science* 326 (2009) 1707-1711.
- [13] E. Zeqiraj, B.M. Filippi, S. Goldie, I. Navratilova, J. Boudeau, M. Deak, D.R. Alessi, D.M. van Aalten, ATP and MO25 $\alpha$  regulate the conformational state of the STRAD $\alpha$  pseudokinase and activation of the LKB1 tumour suppressor, *PLoS Biol.* 7 (2009) e1000126.

- [14] A. Zagorska, E. Pozo-Guisado, J. Boudeau, A.C. Vitari, F.H. Rafiqi, J. Thastrup, M. Deak, D.G. Campbell, N.A. Morrice, A.R. Prescott, D.R. Alessi, Regulation of activity and localization of the WNK1 protein kinase by hyperosmotic stress, *J. Cell Biol.* 176 (2007) 89-100.
- [15] J. van der Wijst, M.G. Blanchard, H.I. Woodroof, T.J. Macartney, R. Gourlay, J.G. Hoenderop, R.J. Bindels, D.R. Alessi, Kinase and channel activity of TRPM6 are coordinated by a dimerization motif and pocket interaction, *Biochem. J.* 460 (2014) 165-175.
- [16] O. Trott, A.J. Olson, AutoDock Vina: improving the speed and accuracy of docking with a new scoring function, efficient optimization, and multithreading, *J. Comput. Chem.* 31 (2010) 455-461.
- [17] C.C. Milburn, J. Boudeau, M. Deak, D.R. Alessi, D.M. van Aalten, Crystal structure of MO25 alpha in complex with the C terminus of the pseudo kinase STE20-related adaptor, *Nat. Struc. Mol. Biol.* 11 (2004) 193-200.
- [18] M.F. Sanner, Python: a programming language for software integration and development, *J. Mol. Graph. Model.* 17 (1999) 57-61.
- [19] S. Sengupta, A. Lorente-Rodriguez, S. Earnest, S. Stippec, X. Guo, D.C. Trudgian, H. Mirzaei, M.H. Cobb, Regulation of OSR1 and the sodium, potassium, two chloride cotransporter by convergent signals, *Proc. Natl. Acad. Sci. USA* 110 (2013) 18826-18831.
- [20] K. Yamada, H.M. Park, D.F. Rigel, et al., Small-molecule WNK inhibition regulates cardiovascular and renal function, *Nat. Chem. Biol.* 12 (2016) 896-898.
- [21] C.M. Chresta, B.R. Davies, I. Hickson, et al., AZD8055 is a potent, selective, and orally bioavailable ATP-competitive mammalian target of rapamycin kinase inhibitor with in vitro and in vivo antitumor activity, *Cancer Res.* 70 (2010) 288-298.
- [22] Y. Mehellou, D.R. Alessi, T.J. Macartney, M. Szklarz, S. Knapp, J.M. Elkins, Structural insights into the activation of MST3 by MO25, *Biochem. Biophys. Res. Comm.* 431 (2013) 604-609.

**Competing Interests:** The authors declare that they have no competing interests.

## Figure legends

**Figure 1. Identification of proteins that bind OSR1 pS339. A.** A general representation of the WNK-signalling cascade. WNK kinases phosphorylate SPAK and OSR1 at many residues on their T-loop and

S-motif. Two phosphorylation sites are most prominent; OSR1 T185 and S325 and SPAK T233 and S373. SPAK and OSR1 phosphorylation at residues S387 and S339, respectively, is poorly understood. WNK-phosphorylated SPAK and OSR1 kinases in complex with the scaffolding protein MO25 phosphorylate a series of sodium, potassium and chloride co-transporters. **B.** Coomassie stained gel of material pulled down from HEK293 cells using the *N*-terminally biotinylated 16-mer phosphopeptide C<sub>12</sub>-TEDGDWEW**p**SDDEMDEK or its corresponding non phosphorylated peptide C<sub>12</sub>-TEDGDWEW**S**DDDEMDEK. These peptides correspond to amino acid residues 379-394 of human SPAK. The *N*-terminally biotinylated 18-mer peptide C<sub>12</sub>-SEEGKPQLVGRFQVTSSK (RFQV peptide) derived from WNK1 (aa. 1006-1023) and empty streptavidin beads were used as controls. The bands that were excised and analysed by mass spec are shown in boxes. **C.** Summary of mass spectrometry results of the proteins identified from every band excised and shown in B. **C.** Confirmation of mass spectrometry results by western blotting. The biotinylated peptides used in the mass spectrometry pulldown experiment were incubated with HEK293 lysates. This was followed by streptavidin-biotin pulldown and western blotting for endogenous MO25 and SPAK. **D.** Fluorescence polarisation (FP) assay of MO25 $\alpha$  binding to the phosphorylated and non-phosphorylated 16-mer WEW peptides. These peptides contained a CCPGCC *N*-terminal tag, which was used in the labelling with Lumio Green™. The fluorescence polarisation was measured using a PheraSTAR (excitation/emission) after the incubation of 10 nM of these peptides with recombinant MO25 $\alpha$  at the indicated concentrations. The assay was run in triplicates. *n* = 3.

**Figure 2. Phosphorylation of SPAK at S387 *in vitro* by WNK kinases.** **A.** *In vitro* kinase assay results showing phosphorylation of SPAK at S387 is not an autophosphorylation site. Recombinant human full length GST-tagged SPAK WT or KD were phosphorylated *in vitro* by recombinant human either GST-tagged WNK1 (1-699) WT or KD using 0.1 mM [ $\gamma$ -<sup>32</sup>P]ATP and 10 mM MgCl<sub>2</sub> at 30 °C for 30 minutes. The material from each sample was then probed for SPAK T233, S373 and S387 phosphorylation by Western blotting. **B.** GST blot showing amounts of proteins (GST-SPAK WT and KD as well as GST WNK1 WT and KD) in each sample of the *in vitro* kinase assay.

**Figure 3. SPAK phosphorylation at S387 is WNK1-dependent.** **A.** HEK293 cells were stimulated with sorbitol or hypotonic low-chloride buffer for the indicated times. The cells were then lysed and subjected to immunoblot analysis with the indicated total and phospho-specific antibodies. \* indicates a non-specific band. **B.** HEK293 cells were treated with low-chloride hypotonic buffer for 15 minutes. Then, they were treated with the WNK-signaling inhibitor WNK463 and the mTORC2 inhibitor AZD8055 at the indicated concentrations.

Following cell lysis, the cell lysates were immunoblotted with the indicated total and phospho-specific antibodies. Similar results were obtained in three separate experiments.

**Figure 4. Binding of SPAK and OSR1 the WEW tripeptide to MO25 $\alpha$ .** **A.** Figure showing the position of the key WEF motif (depicted in pink sticks) of STRAD $\alpha$  in complex with human MO25 $\alpha$  protein (PDB: 1UPK) as reported by Milburn *et al* [17]. **B.** *In silico* docking of the conserved SPAK and OSR1 WEW motif (depicted in yellow sticks) in the human MO25 $\alpha$  protein (PDB: 1UPK). The key four amino acids [K257, R264, K297 and K301 (shown in brown sticks)] that form a pocket in which the WEF/WEW motifs sit have been labelled. The WEF and WEW residues are labelled in red in A and B, respectively. **C.** Overlap of A and B with the key amino acids being labelled. WEF shown in pink sticks and WEW shown in yellow sticks. The part transparent MO25 $\alpha$  protein surface shown. Details of the *in silico* docking are given under Materials and Methods. **D and E.** Effect of MO25 $\alpha$  mutations on the *in vitro* activation of SPAK T233E and OST1 T185E respectively. Recombinant full-length human SPAK T233E and OSR1T185E 1-527 were purified from E.coli and used (0.22  $\mu$ M) with the relevant MO25 $\alpha$  WT or mutants (1  $\mu$ M) to phosphorylate the peptide substrate CATCHtide *in vitro* for 30 minutes at 30 °C. 0.1 mM [ $\gamma$ - $^{32}$ P]-ATP and 10 mM MgCl<sub>2</sub>. The samples were run in triplicates. **F.** Myc-MO25 WT or the indicated mutants were overexpressed in HEK293 cells. Cell lysates (3 mg) were treated with biotinylated peptides (3  $\mu$ g) either phosphorylated (Biotin-C<sub>12</sub>-TEDGDWEWpSDDEMDEK) or non-phosphorylated (Biotin-C<sub>12</sub>-TEDGDWEWSDDDEMDEK). Following streptavidin-biotin pull-down the material underwent blotting for Myc.

Figures:

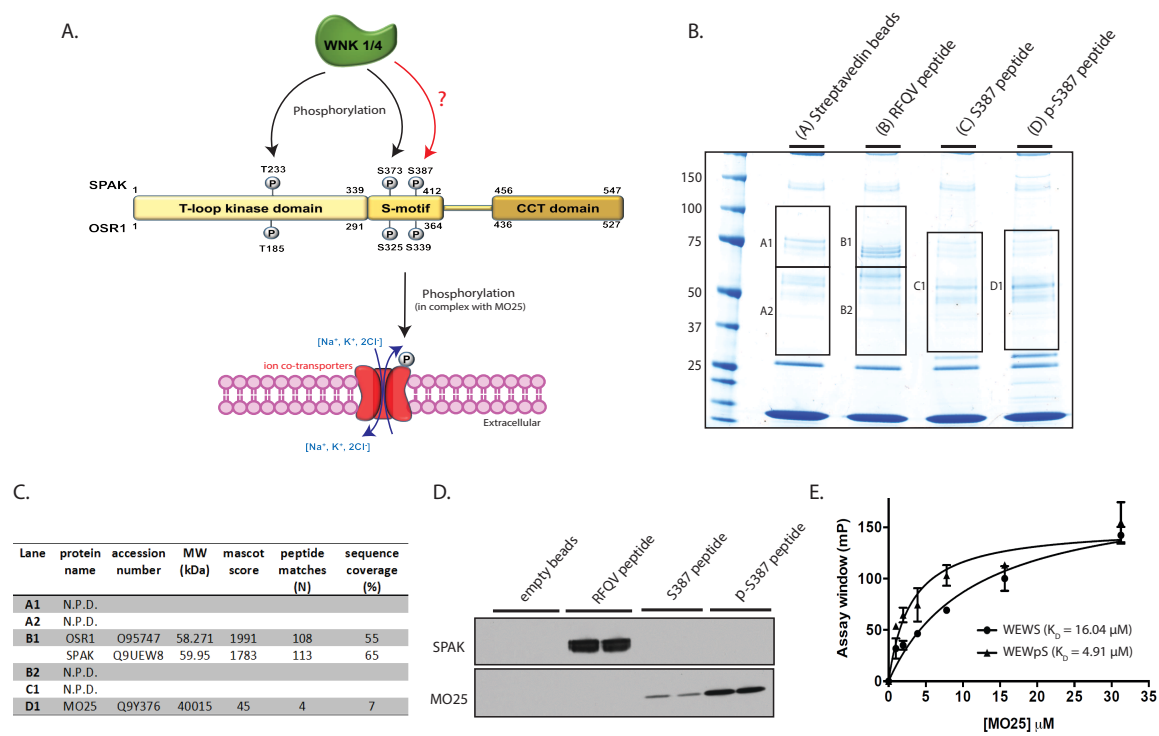
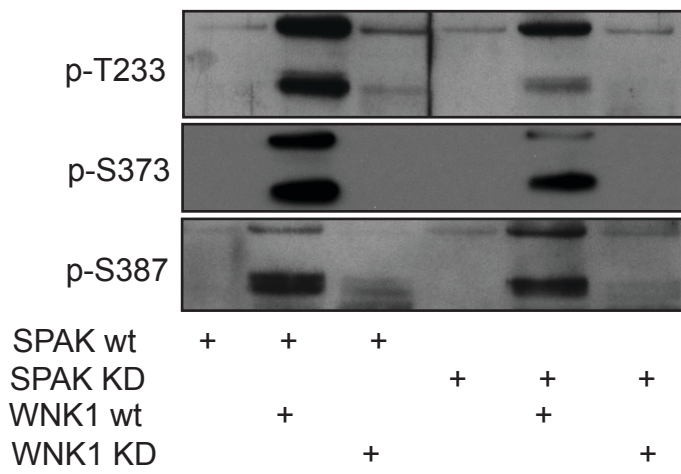


Figure 1

A.



B.

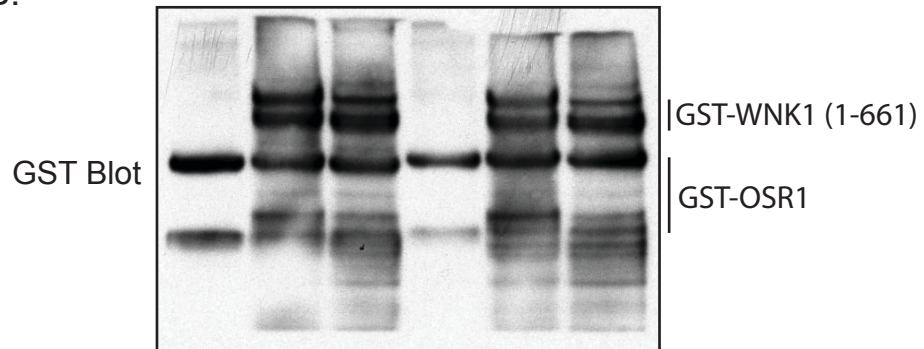
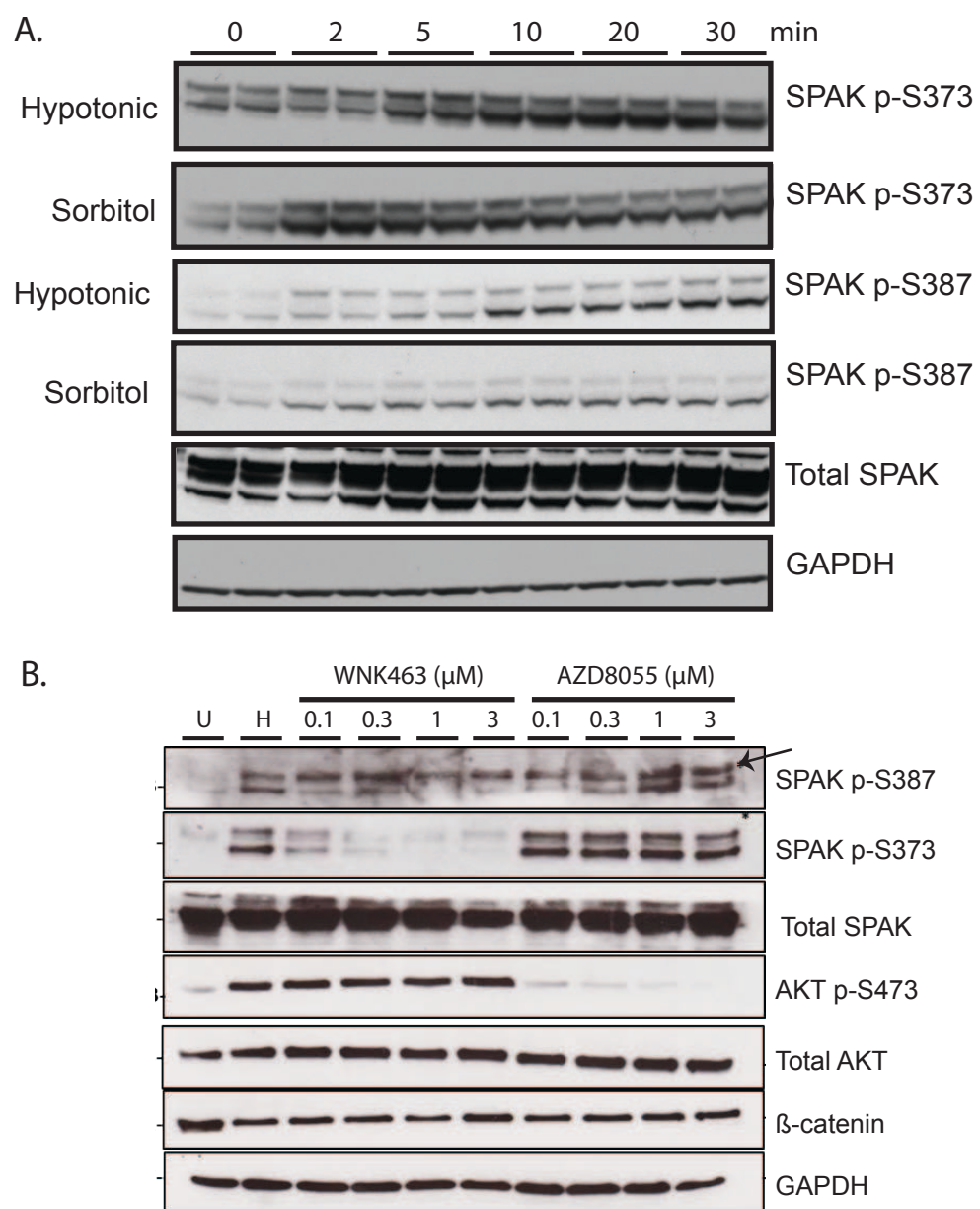
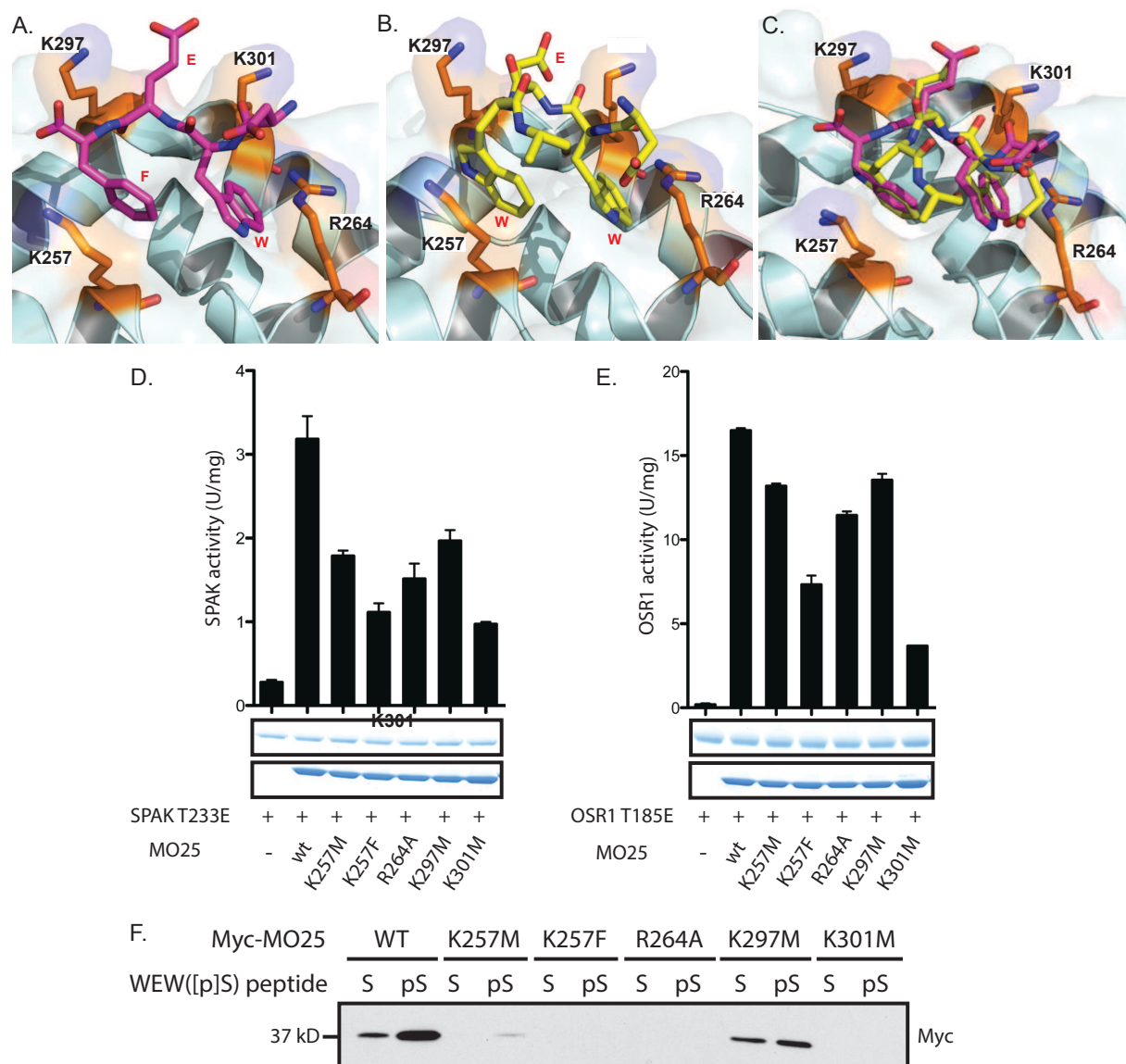


Figure 2



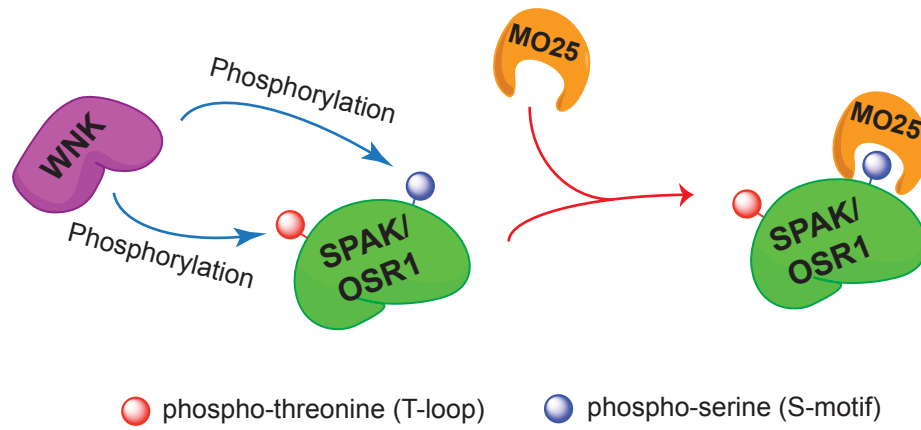
**Figure 3**



**Figure 4**



## Graphical abstract



## Supplementary Material

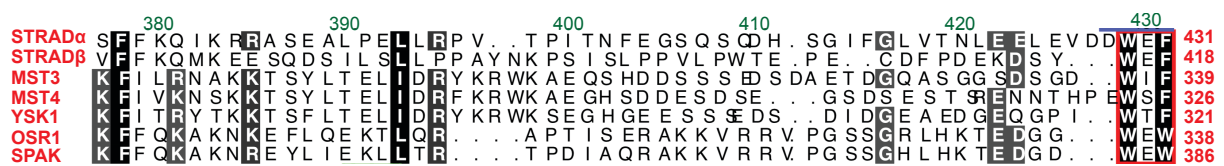
### C-terminal Phosphorylation of SPAK and OSR1 Kinases Promotes Their Binding and Activation by the Scaffolding Protein MO25

Youcef Mehellou,<sup>1,\*</sup> Mubarak A. Alamari,<sup>2</sup> Binar A. Dhiani,<sup>1</sup> Hachemi Kadri<sup>1</sup>

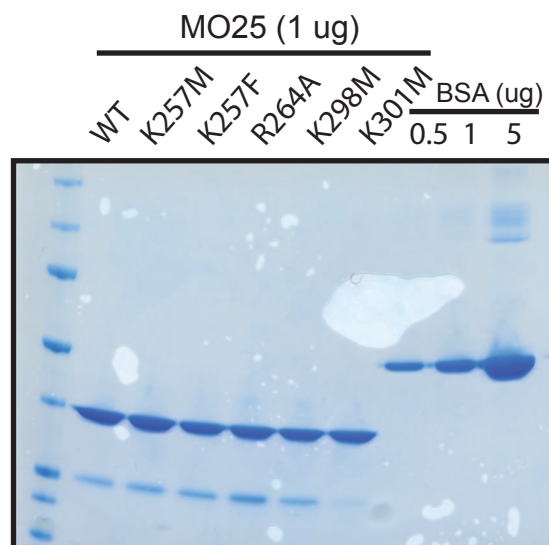
<sup>1</sup>School of Pharmacy and Pharmaceutical Sciences, King Edward VII Avenue, Cardiff University, Cardiff, UK.

<sup>2</sup>School of Pharmacy, College of Medical and Dental Sciences, University of Birmingham, Edgbaston, Birmingham B15 2TT, UK.

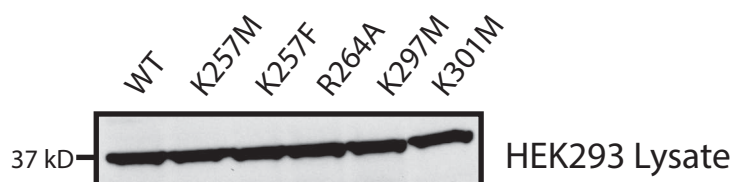
#### 1. Supplementary Figures



**Supplementary Figure S1.** Sequence alignment of the C-terminal domain region that encompasses the WXF/WXW motif (in red box) STE20 kinases that have been reported to bind MO25. Sequence alignment (black = conserved, white = not conserved). This was adapted from Filippi et al [6].



**Supplementary Figure S2.** SDS gel showing the various MO25α wild-type (wt) mutants that were purified from E.coli and used in the in vitro kinase assay shown in Figure 4D and E.



**Supplementary Figure S3.** A Western blot showing the total overexpression levels MO25α wild-type (wt) mutants in HEK293 lysates. 20 µg of total HEK293 cell lysate per sample was used in this Western

blot. Anti-Myc antibody was used. These lysates were subsequently used in the pulldown assay/peptide competition assay shown in Figure 4F.

## **2. Reagents and Standard Protocols**

### **Reagents**

The materials used were sequencing-grade trypsin (Promega); protease-inhibitor cocktail tablets (Roche); Protein G–Sepharose and all chromatography media (GE Healthcare Life sciences); Tween 20, Colloidal Blue staining kit and precast SDS polyacrylamide BisTris gels (Invitrogen); Nonidet P40 (Fluka); ampicillin (Merck); imidazole and DL-Dithiothreitol [DTT] (Sigma); P81 phosphocellulose (Whatman); [ $\gamma$ - $^{32}$ P]-ATP (Perkin Elmer). All peptides were synthesised by GLS Peptide Synthesis.

### **DNA plasmids**

Cloning, restriction enzyme digests, DNA ligations and other recombinant DNA procedures were performed using standard protocols. All mutagenesis reactions were performed using KOD polymerase (Novagen) followed by digestion of the product with DpnI. All the clones were provided by the Division of Signal Transduction Therapy (DSTT), Dundee. The DNA accession numbers as well as the DSTT DNA code (DU) number for all proteins used in this study are: human GST-MO25 $\alpha$  (NP\_057373; DU2945), GST-Myc-MO25 $\alpha$  (DU30906), GST-MYC-MO25 $\alpha$  K257M (DU44511), GST-MYC-MO25 $\alpha$  K257F (DU44512); GST-MYC-MO25 $\alpha$  R264A (DU44513), GST-MYC-MO25 $\alpha$  K297M (DU44514); GST-MYC-MO25 $\alpha$  K301M (DU44515), GST-HA-OSR-T185E (NP\_005100; DU6131), GST-HA-SPAK-T233E (NP\_005100; DU6131), GST-SPAK (AAC72238.1; DU41756), GST-HA-SPAK D212/A (AF099989, DU6013), GST-WNK1 [1-661] (Q9H4A3; DU43603), GST-WNK1 kinase dead [1-661] (Q9H4A3; DU43603). DNA constructs used for transfection were purified from DH5 $\alpha$  strain of *E. coli* using Qiagen Plasmid kits according to the manufacturer's protocol. All DNA constructs were verified by DNA sequencing performed by DNA Sequencing & Services (MRCPPU, College of Life Sciences, University of Dundee, UK; [www.dnaseq.co.uk](http://www.dnaseq.co.uk)) using Applied Biosystems Big-Dye Version 3.1 chemistry on an Applied Biosystems model 3730 automated capillary DNA sequencer. All protein concentrations were determined using a Bradford method kit (Bio-Rad). The purity of all proteins was assessed by SDS–polyacrylamide gel electrophoresis. Sequence alignments were performed using MUSCLE [1], which were edited and displayed using the program ALINE [2].

### **Antibodies**

The antibodies against the following antigens were raised in sheep and affinity-purified on the appropriate antigen by the Division of Signal Transduction Therapy Unit at the University of Dundee: SPAK total antibody (full-length human SPAK protein, catalogue number S637B), SPAK/OSR1n(S-motif) phosphoS387/S339 (human SPAK residues 380-394: EDGDWEWS\*DDEMDEK), which is highly similar to residues 332-346 of human OSR1 (EDGGWEWS\*DDEFDEE). The SPAK/OSR1 (T-loop) phosphoThr233/T185 (S240C), SPAK/OSR1 (S-motif) phospho-Ser373/S325 (S670B) were produced as reported previously[3]. Total MO25 $\alpha$  (cat. No. 2716) and the anti-GAPDH (glyceraldehyde-3-phosphate dehydrogenase) were purchased from Cell Signalling Technology. Anti-Myc antibody (C3956) was purchased from Sigma. Horseradish peroxidase (HRP)-conjugate anti-GST (ab58626) antibody was purchased from Abcam, and the secondary antibodies coupled to HRP used for immunoblotting were obtained from Pierce.

### **Buffers**

Buffer A contained 50 mM Tris/HCl (pH 7.5), 0.1 mM EGTA and 1 mM DTT (dithiothreitol). The mammalian cells lysis buffer contained 50 mM Tris/HCl (pH 7.5), 0.15 M NaCl, 1 mM EGTA, 1 mM EDTA, 1 mM Na<sub>3</sub>VO<sub>4</sub>, 50 mM NaF, 5 mM Na<sub>4</sub>P<sub>2</sub>O<sub>7</sub>, 0.27 M sucrose, 1% (w/v) Nonidet P40, 1 mM benzamidine, 0.1 mM PMSF, 0.1% 2-mercaptoethanol and Roche protease inhibitor mix (1 tablet in

50 ml). Low-salt buffer contained 50 mM Tris-HCl, pH 7.8, 150 mM NaCl, 5% (v/v) glycerol, 0.2 mM EDTA, 0.2 mM EGTA, 1 mM benzamidine, 20 mM imidazole and 0.075% (v/v)  $\beta$ -mercaptoethanol. TTBS (Tris-buffered saline containing Tween 20) was Tris/HCl (pH 7.5), 0.15 M NaCl and 0.2% Tween 20. SDS sample buffer was 1×NuPAGE LDS (lithium dodecyl sulfate) sample buffer (Invitrogen), containing 1% (v/v) 2-mercaptoethanol. Bacterial lysis buffer contained 50 mM Tris/HCl (pH 7.5), 0.15 M NaCl, 1 mM EGTA, 1 mM EDTA, 0.27 M sucrose, 1% (w/v) Triton X-100, 0.1 mM PMSF, 1 mM benzamidine, 0.5 mg/ml lysozyme and 0.015 mg/ml DNase containing 1% (v/v) 2-mercaptoethanol. Basic control buffer contains 135 mM NaCl, 5 mM KCl, 0.5 mM  $\text{CaCl}_2$ , 0.5 mM  $\text{MgCl}_2$ , 0.5 mM  $\text{Na}_2\text{HPO}_4$ , 0.5 mM  $\text{Na}_2\text{SO}_4$  and 15 mM HEPES (pH 7.0). Hypotonic low-chloride buffer contains 67.5 mM sodium gluconate, 2.5 mM potassium gluconate, 0.25 mM  $\text{CaCl}_2$ , 0.25 mM  $\text{MgCl}_2$ , 0.5 mM  $\text{Na}_2\text{HPO}_4$ , 0.5 mM  $\text{Na}_2\text{SO}_4$  and 7.5 mM HEPES (pH 7.0).

### ***Cell culture***

HEK 293 cells were cultured in DMEM (Dulbecco's modified Eagle's medium) supplemented with 10% (v/v) foetal bovine serum, 2 mM *L*-glutamine, 100 units/mL penicillin and 0.1 mg/mL streptomycin. For transient transfection experiments, adherent HEK-293 cells were transfected with 20  $\mu\text{L}$  of 1 mg/mL poly(ethylenimine) (Polysciences) and 5–10  $\mu\text{g}$  of plasmid DNA as described previously [4]. In cases where stimulation was needed, cells were stimulated with either basic or hypotonic low chloride or hypertonic conditions for 30 min. Following lysis, the lysates were clarified by centrifugation at 26,000 *g* for 15 min and the supernatants were frozen in aliquots (100  $\mu\text{L}$ ) in liquid nitrogen and stored at  $-80^\circ\text{C}$ . Protein concentrations were determined using the Bradford method [5].

### ***Immunoprecipitation***

For the immunoprecipitation, GST glutathione-sepharose beads were used. The antibodies were covalently coupled to Protein G-Sepharose employing dimethyl pimelimidate at a ratio of 1  $\mu\text{g}$  of antibody per 1  $\mu\text{L}$  of beads. For immunoprecipitation, 0.2–5 mg of lysates were incubated with 5–10  $\mu\text{L}$  of antibody-resin conjugate for 1 h at  $4^\circ\text{C}$  with gentle agitation, and the immunoprecipitates were then washed three times with 1 mL of lysis buffer containing 0.5 M NaCl and then twice with 1 mL of Buffer A. Proteins were eluted by resuspending the washed immunoprecipitates in 20–100  $\mu\text{L}$  of 1 × SDS sample buffer.

### ***Immunoblotting***

Samples were heated in sample buffer, subjected to SDS/PAGE and transferred on to nitrocellulose membranes. Membranes were blocked for 30 min in TBST, containing 5% (w/v) dried skimmed milk. The membranes were then incubated overnight at  $4^\circ\text{C}$  in TBST containing 5% (w/v) skimmed milk with the indicated primary antibody. Sheep antibodies were used at a concentration of 1–2  $\mu\text{g}/\text{mL}$ , whereas commercial antibodies were diluted 1,000–2,000-fold. The incubation with phosphospecific sheep antibodies was performed with the addition of 10  $\mu\text{g}/\text{mL}$  of the dephosphopeptide antigen used to raise the antibody. The blots were then washed three times with TTBS and incubated for 1 h at room temperature ( $25^\circ\text{C}$ ) with secondary HRP-conjugated antibodies diluted 2500-fold in 5% (w/v) skimmed milk in TTBS. After repeating the washing steps, the signal was detected with the enhanced chemiluminescence reagent. Immunoblots were developed using a film automatic processor (SRX-101, Konica Minolta Medical), and films were scanned with at 300-d.p.i. resolution on a scanner (V700 PHOTO, Epson).

### ***In vitro kinase assay***

The catalytic activity of SPAK and OSR1 was determined in vitro using [ $\gamma$ - $^{32}\text{P}$ ]ATP as reported [6]. Phosphotransferase activity of SPAK and OSR1 was measured in a total assay volume of 50  $\mu\text{L}$ .

consisting of 50 mM TrisHCl (pH 7.5), 0.1 mM EGTA, 0.1% (v/v) 2-mercaptoethanol, 10 mM MgCl<sub>2</sub>, 0.1 mM [ $\gamma$ -<sup>32</sup>P]ATP (200 c.p.m./pmol). The assays were carried out at 30 °C and were terminated after 30 min by applying 40  $\mu$ L of the reaction mixture onto P81 membranes. These were washed in phosphoric acid, and the incorporated radioactivity was measured by scintillation counting as described previously for MAP kinase [7]. One unit (U) of activity represents the incorporation to the substrate of 1 nmol of  $\gamma$ -<sup>32</sup>P per minute.

## References

- [1] R.C. Edgar, MUSCLE: multiple sequence alignment with high accuracy and high throughput, *Nucleic Acids Res.* 32 (2004) 1792-1797.
- [2] C.S. Bond, A.W. Schuttelkopf, ALINE: a WYSIWYG protein-sequence alignment editor for publication-quality alignments, *Acta Crystallogr. D Biol. Crystallogr.* 65 (2009) 510-512.
- [3] A. Zagorska, E. Pozo-Guisado, J. Boudeau, A.C. Vitari, F.H. Rafiqi, J. Thastrup, M. Deak, D.G. Campbell, N.A. Morrice, A.R. Prescott, D.R. Alessi, Regulation of activity and localization of the WNK1 protein kinase by hyperosmotic stress, *J. Cell Biol.* 176 (2007) 89-100.
- [4] Y. Durocher, S. Perret, A. Kamen, High-level and high-throughput recombinant protein production by transient transfection of suspension-growing human 293-EBNA1 cells, *Nucleic Acids Res.* 30 (2002) E9.
- [5] M.M. Bradford, A rapid and sensitive method for the quantitation of microgram quantities of protein utilizing the principle of protein-dye binding, *Analytical biochemistry*, 72 (1976) 248-254.
- [6] B.M. Filippi, P. de los Heros, Y. Mehellou, I. Navratilova, R. Gourlay, M. Deak, L. Plater, R. Toth, E. Zeqiraj, D.R. Alessi, MO25 is a master regulator of SPAK/OSR1 and MST3/MST4/YSK1 protein kinases, *EMBO J.* 30 (2011) 1730-1741.
- [7] D.R. Alessi, A. Cuenda, P. Cohen, D.T. Dudley, A.R. Saltiel, PD 098059 is a specific inhibitor of the activation of mitogen-activated protein kinase kinase in vitro and in vivo, *J. Biol. Chem.* 270 (1995) 27489-27494.